Dynamics of Disordered Spin Systems

DAD / PAF

PhD defense of D. A. Drabold
January, 1989
Washington University (St Louis)

Outline :

I. Spin Dynamics
theoretical generalities
+ link to experiment

Blow up! PR xerox — no words

II. Disorder / Dilution ← (more specific)
Effects of random dilution [fluct dissip thm]

III. Realistic Calculations
recent developments

[additional terminology in moments (any pdf)]
Entropy $\mathcal{H}$?
{Localization — band edge}

IV. Hydrogen (if there is time!)

I. Spin Dynamics

Hamiltonian:

$$\mathcal{H} = \sum_{\substack{\alpha\beta \\ i\neq j}} A_\alpha(i)\, \Xi_{\alpha\beta}(ij)\, A_\beta(j)$$

irreducible multipole operators [operator analogues to Y_{lm}]

General coupling between sites and operators

Greek: index spin operator type
Latin: index site

Example: Choose $\Xi_{\alpha\beta}(ij) = J_{ij}\{\delta_{\alpha 0}\delta_{\beta 0} - \delta_{\beta 1}\delta_{-1\alpha} - \delta_{-1\beta}\delta_{1\alpha}\}/4$

$$\Rightarrow \mathcal{H} = \sum_{i\neq j} J_{ij}\, \vec{S}_i \cdot \vec{S}_j$$

Heisenberg Exchange

Time Evolution:

$$A_\alpha(t) \equiv e^{i\mathcal{H}t} A_\alpha e^{-i\mathcal{H}t}$$

$$i\frac{d}{dt}A_\alpha(t) = [A_\alpha(t), \mathcal{H}] = \sum_{\beta\gamma} \Omega_{\alpha\beta\gamma}(ij) A_\beta(i) A_\gamma(j)$$

But we can almost never solve this!

⟨ Ising model ⟩

"Equation of motion" closure

Link to the Real World

experiment measures DYNAMICAL SPIN CORRELATION FUNCTIONS or consequences thereof.

$$G_{\alpha}(i,t) \equiv \Theta(t) \left\langle \theta(i,t)\, \theta^{+}(i,0) \right\rangle$$

- Θ: Heaviside unit step fcn [causality]
- $\theta(i,t)$: a spin operator at time t, site i
- $\langle \cdot \rangle$: thermal average. $T = \infty$ assumed ($k_B T \gg$ magnetic energies)

Examples: Think of a system of coupled dipoles:

T_1 relaxation: $\theta = \sum_{i=1}^{N} A_{10}(i) \sim \sum_{i=1}^{N} S_z(i)$

T_2 relaxation $\theta = \sum_{i=1}^{N} A_{11}(i) \sim \sum_{i=1}^{N} S_+(i)$

NMR absorption spectrum ↔ [watch Dephasing]

A Central problem of Theory: Get G from $\mathcal{H}$.

How!?

1. Simply Diagonalize $\mathcal{H}$.

If $\mathcal{H}|n\rangle = \epsilon_n |n\rangle$ then

$T = \infty$

$$G_\alpha(t) = \theta(t)\langle A_\alpha(t) A_\alpha^\dagger \rangle$$

$$= \theta(t) \sum_{mn} |\langle m | A_\alpha | n \rangle|^2 e^{it\{\epsilon_m - \epsilon_n\}\hbar^{-1}} \quad \{1 = \sum_n |m\rangle\langle n|\}$$

But $\dim\{\mathcal{H}\} \sim 2^N$ N = # spins.

Can't explicitly diagonalize for $N \gtrsim 10$.

2. Moments {sum rules}

trace invariance & operator identities like

$$\frac{\langle n|\theta\mathcal{H}|m\rangle}{\langle n|\theta|m\rangle} = \epsilon_m \Rightarrow$$

We can get $\langle \omega^n \rangle \equiv \int_{-\infty}^{\infty} G(\omega)\omega^n d\omega$, $G(\omega) = \mathcal{F}\{G(t)\}$.

How to calculate moments

(i) brute force — $\frac{d^n G(t)}{dt^n}\Big|_{t=0}$

$$G(t) = \sum_{n=0}^{\infty} M_n \frac{(it)^n}{n!}$$

M_n moments

[Taylor coefficients in t-domain
moments in ω]

Def^n of G + Heisenberg eq. of motion imply

$$M_n \sim \left\langle \left[\cdots \left[\left[\left[A_\alpha, \mathcal{H} \right], \mathcal{H} \right], \mathcal{H} \right] \cdots \right] A_\alpha^\dagger \right\rangle$$

(n times)

(for me)

This is tedious (and impossible for $n \gtrsim 6$ and a nontrivial interaction)

(ii) diagrammatic approach
[Bookkeeping]

introduce vertex

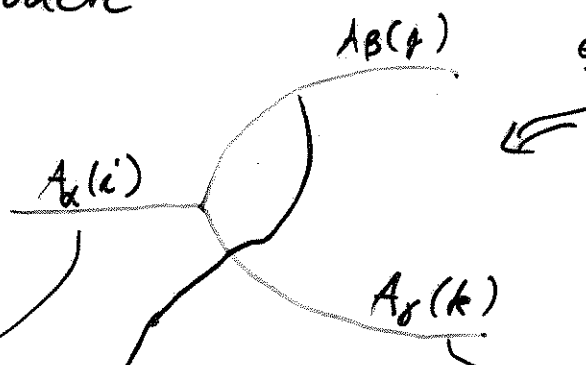

elegant derivation:
Matrix ele. of Liouville op in dual space, Lie groups etc. Reiter

$\equiv \Omega_{\alpha\beta\gamma}(ijk)$ ⇐ Analytic expression

{ Ω satisfies $i\frac{dA_\alpha(t)}{dt} = \sum_{\beta\gamma} \Omega_{\alpha\beta\gamma}(ij) A_\beta(i) A_\gamma(j)$ }

One can show that moments M_n are given by closed, distinct graphs:

$$M_2^{\alpha\beta}(i,j) = \sum_{\text{internal lines}}$$

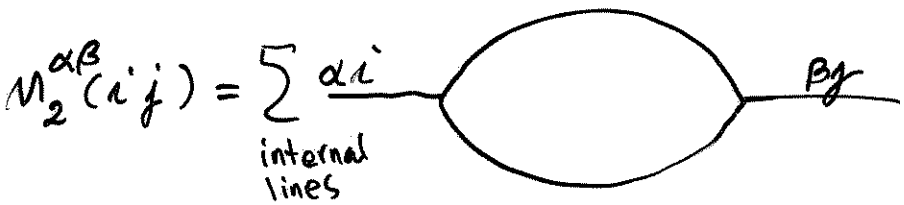

$$M_4^{\alpha\beta}(i,j) = \sum_{\text{internal lines}}$$

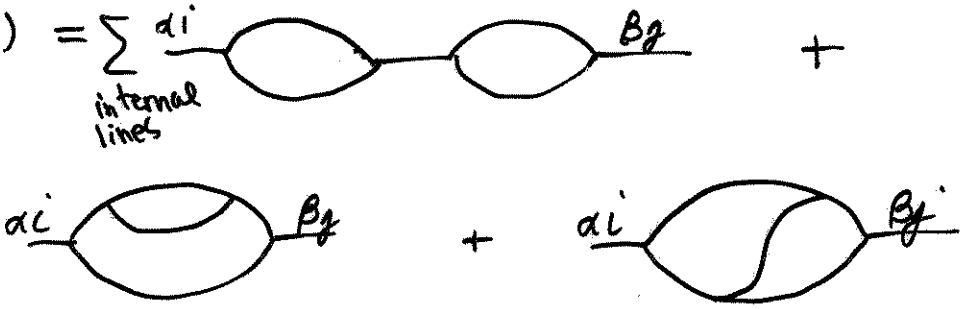

∴ [internal lines are left unlabelled because there are many decorations]

Diagrammology

Leads to simple, general way to calculate moments

$\forall\ \exists$: (transp$^{\text{xenox}}$)

---

* In practice can only calculate a few M_n : Taylor series is valid for <u>short times only</u> !

$$M_4^{(1,m)}(ii) = \Omega_{1m,2\mu,2\nu}(ij)\,\Omega_{2\nu,1\lambda,2\chi}(jk)\,\Omega^*_{2\eta,1\lambda,2\chi}(jk)\,\Omega^*_{1m,2\mu,2\eta}(ij) + \Omega_{1m,2\mu,2\nu}(ij)\,\Omega_{2\mu,1\lambda,2\chi}(ik)\,\Omega^*_{2\eta,1\lambda,2\chi}(ik)\,\Omega^*_{1m,2\eta,2\nu}(ij)$$
$$+ \Omega_{1m,2\mu,2\nu}(ij)\,\Omega_{2\mu,1\lambda,2\chi}(ik)\,\Omega^*_{2\eta,1\lambda,2\nu}(ij)\,\Omega^*_{1m,2\eta,2\chi}(ik) + \Omega_{1m,2\nu,2\mu}(ij)\,\Omega_{1\lambda,2\eta,2\chi}(ij)\,\Omega^*_{1\lambda,2\mu,2\nu}(ij)\,\Omega^*_{1m,2\chi,2\eta}(ij)$$
$$+ \Omega_{1m,2\mu,2\nu}(ij)\,\Omega_{1\lambda,2\eta,2\chi}(ik)\,\Omega^*_{1\lambda,2\mu,2\nu}(ij)\,\Omega^*_{1m,2\eta,2\chi}(ik)$$

and

$$M_4^{2,m}(ii) = \Omega_{2m,1\lambda,2\mu}(ik)\,\Omega_{1\lambda,2\nu,2\chi}(ij)\,\Omega^*_{1\psi,2\nu,2\chi}(ij)\,\Omega^*_{2m,1\psi,2\mu}(ik) + \Omega_{2m,1\lambda,2\mu}(ij)\,\Omega_{1\lambda,2\nu,2\chi}(ik)\,\Omega^*_{1\psi,2\nu,2\mu}(ij)\,\Omega^*_{2m,1\psi,2\chi}(ik)$$
$$+ \Omega_{2m,1\lambda,2\mu}(ij)\,\Omega_{2\mu,1\psi,2\chi}(jk)\,\Omega^*_{2\nu,1\psi,2\chi}(jk)\,\Omega^*_{2m,1\lambda,2\nu}(ij) + \Omega_{2m,1\lambda,2\mu}(ij)\,\Omega_{2\nu,1\psi,2\chi}(ik)\,\Omega^*_{2\nu,1\lambda,2\mu}(ij)\,\Omega^*_{2m,1\psi,2\chi}(ik),$$

where sums are implicit on all indices other than i and m, and $-2 \le \mu,\nu,\chi,\eta \le 2$, $-1 \le \lambda,\ \psi \le 1$, and $j \neq k$ except for the last term in each of the previous equations, where j and k can be identical. Note that these expressions are readily rewritten in analytical forms involving the function $F_{mn}(i,j)$ of Ref. 7. Further, it is simple to code these expressions in the form of the vertices to obtain moments for a given configuration of impurities: This is useful for calculating T_1 for random mixtures of ortho- and para-H_2, for example.[6-9]

IV. CONCLUSIONS

We have obtained general expressions for the first two nontrivial moments of resonant absorption spectra which should be of interest for magnetic resonance work. The method we have developed yields expressions convenient for practical use with a minimum of detailed commutator algebra. We should also remark that this analysis is not limited to spin systems: Similar equations must hold for more general bilinear Hamiltonians.

ACKNOWLEDGMENTS

This work owes much to Professor Peter Fedders. The author also wishes to acknowledge helpful conversations with Professor R. E. Norberg, Professor Mark Conradi, and Dr. Ronald Fisch. This work was supported in part by the National Science Foundation-Low Temperature Physics Program, under Grant No. DMR 85-03083.

[1] C. W. Myles and P. A. Fedders, Phys. Rev. B **9**, 4872 (1974).
[2] G. F. Reiter, Phys. Rev. B **5**, 222 (1972).
[3] A. Abragam, *The Principles of Nuclear Magnetism* (Oxford Univ. Press, New York, 1961).
[4] P. A. Fedders and A. E. Carlsson, Phys. Rev. B **32**, 229 (1985).
[5] A. Abragam and M. Goldman, *Nuclear Magnetism: Order and Disorder* (Oxford Univ. Press, New York, 1982).
[6] A. B. Harris, Phys. Rev. B **2**, 3495 (1970).
[7] C. W. Myles and C. Ebner, Phys. Rev. B **12**, 1638 (1975).
[8] J. Hama, T. Inuzuka, and T. Nakamura, Prog. Theor. Phys. **48**, 1769 (1972).
[9] D. A. Drabold and P. A. Fedders (unpublished).

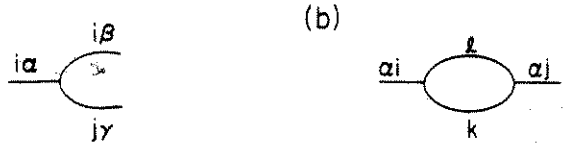

FIG. 1. (a) Basic vertex from which M_n and L_n are constructed. (b) Graph from which second moment is obtained.

FIG. 2. (a) Corresponds to first term of Eq. (8); (b) corresponds to second term of Eq. (8).

The moments of these functions are given by

$$L_n^{\alpha}(ij)=\int_{-\infty}^{\infty}\frac{d\omega}{\pi}\omega^{n-2}\Gamma_{ij}^{\alpha}(\omega),\quad n\geq 2\ ,$$
$$M_n^{\alpha}(ij)=\int_{-\infty}^{\infty}\frac{d\omega}{\pi}\omega^{n}A_{ij}^{\alpha}(\omega),\quad n\geq 0\ . \tag{7}$$

General considerations from analytic function theory imply that knowledge of $\Gamma(A)$ completely specifies $\Sigma(G)$. Reiter and others have shown [1,2] that the moments M_n and L_n are expressible as a sum of graphs constructed from vertices of the type illustrated in Fig. 1(a). It has been shown that the second moment can be represented as the sum of all topologically distinct[2] graphs of the type indicated in Fig. 1(b), where the internal-site indices must be summed over. Note that we did not explicitly attach operator indices to the internal lines: In applying Reiter's method, it is necessary to write down and evaluate each graph form [Fig. 1(b)] producing each graph with distinct operator labels separately.

While explicitly writing out all internal operator lines is practical for some simple Hamiltonians, this becomes quite laborious for complicated interactions, even for the second moment, if the structure of the graphs is not strongly constrained. To illustrate this point, consider the EQQ Hamiltonian. In this case, 30 distinct graphs must be considered for the second moment for each Green's function. There are very many more graphs for the fourth moment. A simple way to alleviate this proliferation of diagrams is to take a different point of view. It is possible to construct the moments by writing out all possible internal-site lines explicitly, and summing only on operator indices for the internal lines. The second moment can then be expressed as

$$M_2^{\alpha}(ij)=L_2^{\alpha}(ij)=\delta_{ij}\sum_{k,\beta,\gamma}\Omega_{\alpha\beta\gamma}(ik)\,\Omega^{*}_{\alpha\beta\gamma}(ik)+\sum_{\beta,\gamma}\Omega_{\alpha\gamma\beta}(ij)\,\Omega^{*}_{\alpha\beta\gamma}(ij)\ . \tag{8}$$

In this and future equations, an asterisk denotes complex conjugate. The first term of Eq. (8) corresponds to Fig. 2(a), the second to Fig. 2(b). While this approach is completely equivalent to Reiter's method, it enables us to obtain such general representations for moments as in Eq. (8). For the fourth moment we use the same method, but the number of graphs involved is too great to reproduce here. We will just observe that the self-energy moment $L_4^{\alpha}(i,j)$ is made up of graphs of the variety depicted in Fig. 3. We show examples of the bubble diagrams [Fig. 3(a)] and vertex corrections [Fig. 3(b)]. There are 8 distinct bubbles and 16 vertex corrections for the fourth moment. Adding up all of these contributions, we obtain the following formidable looking expression for the fourth self-energy moment

$$\begin{aligned}
L_4^{\alpha}(ij)=&[(\alpha\beta\gamma ij)(\beta\delta\epsilon ik)(\zeta\delta\epsilon ik)^{*}(\alpha\zeta\gamma ij)^{*}+(\alpha\gamma\beta ij)(\beta\delta\epsilon jk)(\zeta\delta\epsilon jk)^{*}(\alpha\gamma\zeta ij)^{*}\\
&+(\alpha\gamma\beta ij)(\beta\epsilon\delta jk)(\zeta\delta\epsilon jk)^{*}(\alpha\gamma\zeta ik)^{*}+(\alpha\beta\gamma ij)(\gamma\delta\zeta jk)(\epsilon\beta\delta ij)^{*}(\alpha\epsilon\zeta ik)^{*}\\
&+(\alpha\gamma\beta ij)(\gamma\delta\zeta ik)(\epsilon\delta\beta ij)^{*}(\alpha\epsilon\zeta ik)^{*}+(\alpha\gamma\beta ij)(\gamma\zeta\delta ik)(\epsilon\beta\delta jk)^{*}(\alpha\zeta\epsilon ji)^{*}\\
&+(\alpha\beta\gamma ij)(\gamma\zeta\delta jk)(\epsilon\beta\delta ik)^{*}(\alpha\epsilon\zeta ij)^{*}+(\alpha\gamma\beta ij)(\gamma\zeta\delta ik)(\epsilon\delta\beta jk)^{*}(\alpha\zeta\epsilon ki)^{*}]\delta_{ij}\\
&+(\alpha\gamma\beta ij)(\beta\delta\epsilon jk)(\zeta\delta\epsilon jk)^{*}(\alpha\zeta\gamma ij)^{*}+(\alpha\beta\gamma ij)(\beta\delta\epsilon ik)(\zeta\delta\epsilon ik)^{*}(\alpha\gamma\zeta ij)^{*}\\
&+(\alpha\gamma\beta ik)(\beta\epsilon\delta jk)(\zeta\delta\epsilon jk)^{*}(\alpha\zeta\gamma ij)^{*}+(\alpha\beta\gamma ij)(\beta\delta\epsilon ik)(\zeta\epsilon\delta ik)^{*}(\alpha\gamma\zeta jk)^{*}\\
&+(\alpha\beta\gamma ik)(\beta\delta\epsilon ij)(\zeta\epsilon\delta ij)^{*}(\alpha\zeta\gamma jk)^{*}+(\alpha\beta\gamma ik)(\gamma\delta\zeta jk)(\epsilon\delta\beta ik)^{*}(\alpha\zeta\epsilon kj)^{*}\\
&+(\alpha\beta\gamma ik)(\gamma\zeta\delta jk)(\epsilon\delta\beta ij)^{*}(\alpha\epsilon\zeta jk)^{*}+(\alpha\gamma\beta ik)(\gamma\delta\zeta ij)(\epsilon\beta\delta ik)^{*}(\alpha\zeta\epsilon kj)^{*}\\
&+(\alpha\beta\gamma ik)(\gamma\delta\zeta kj)(\epsilon\beta\delta ik)^{*}(\alpha\zeta\epsilon ij)^{*}+(\alpha\beta\gamma ij)(\gamma\zeta\delta kj)(\epsilon\delta\beta ik)^{*}(\alpha\zeta\epsilon kj)^{*}\\
&+(\alpha\gamma\beta ij)(\gamma\zeta\delta ik)(\epsilon\beta\delta jk)^{*}(\alpha\epsilon\zeta ij)^{*}+(\alpha\beta\gamma ij)(\gamma\zeta\delta jk)(\epsilon\beta\delta ik)^{*}(\alpha\zeta\epsilon ij)^{*}\\
&+(\alpha\gamma\beta ik)(\gamma\zeta\delta ij)(\epsilon\delta\beta jk)^{*}(\alpha\epsilon\zeta ij)^{*}+(\alpha\gamma\beta ik)(\gamma\delta\zeta ij)(\epsilon\delta\beta ik)^{*}(\alpha\zeta\epsilon ij)^{*}\\
&+(\alpha\beta\gamma ij)(\gamma\delta\zeta jk)(\epsilon\delta\beta ij)^{*}(\alpha\epsilon\zeta jk)^{*}+(\alpha\gamma\beta ij)(\gamma\delta\zeta ik)(\epsilon\beta\delta ij)^{*}(\alpha\epsilon\zeta jk)^{*}\ ,
\end{aligned} \tag{9}$$

where for brevity $(\alpha\beta\gamma ij)\equiv\Omega_{\alpha\beta\gamma}(ij)$, and sums are implicit on β, γ, δ, ϵ, ζ, k, and j in the diagonal part. The Van Vleck fourth moment is

$$M_4^{\alpha}(ij)=L_4^{\alpha}(ij)+\sum_{\delta,k}M_2^{\alpha\delta}(ik)M_2^{\delta\alpha}(kj),\quad \text{for } M_2^{\alpha\delta}(ij)=\delta_{ij}\sum_{\beta,\gamma,k}(\alpha\beta\gamma ik)(\delta\beta\gamma ik)^{*}+\sum_{\beta,\gamma}(\alpha\gamma\beta ij)(\delta\beta\gamma ij)^{*}\ .$$

II) Dilution

Consider a lattice. Let prob(occupation) = c.

central theoretical problem : What does dilution do to G ?

x = spin ½ particle

Two limits :

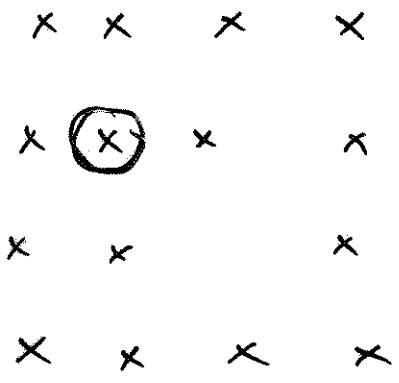

[+]

[B]

What is the NMR spectrum $[G_{11}(\omega)]$ for these?

Intuitive argument :

[A] : ref spin has lots of neighbors

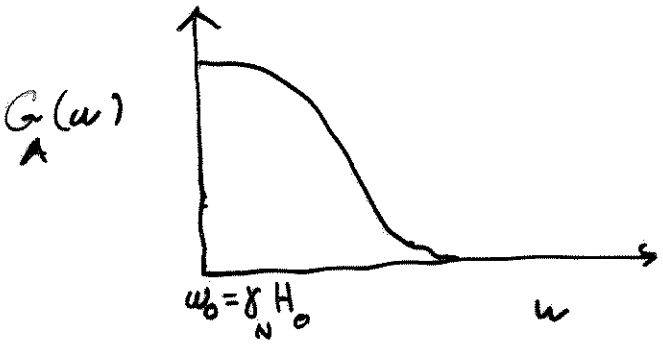

- frequent mutually induced transition
- delocalized spin wavefcn
- "homogeneous broadening"
- Average moments
  {Find "average site", calculate G for this}

[B] : ref spin dominated by one other spin

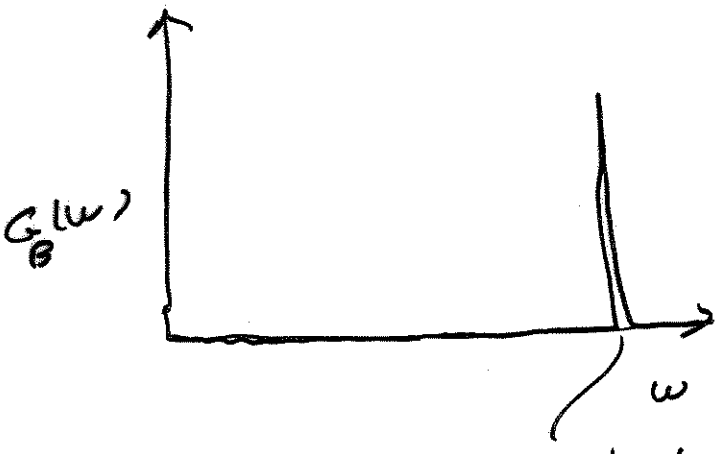

- spin wf is localized at its site
- "inhomogeneous broad."
- pair theory

$\omega_d \sim \gamma_N^2 \hbar / r^{+3}$

A Simplified model to clarify localization; homog. & inhomo. broadening.

Consider an effective field model for $S=\frac{1}{2}$:

$$\omega(t) = \sum_{i=1}^{N} \omega_i \, \xi_i(t)$$

- N: Number of interacting spins
- ω_i: frequency coupling between reference spin and spin # i.
- $\xi_i(t)$: stochastic process [random telegraph] $\{\xi = \pm 1$, ξ Markoff with rate $\gamma\}$

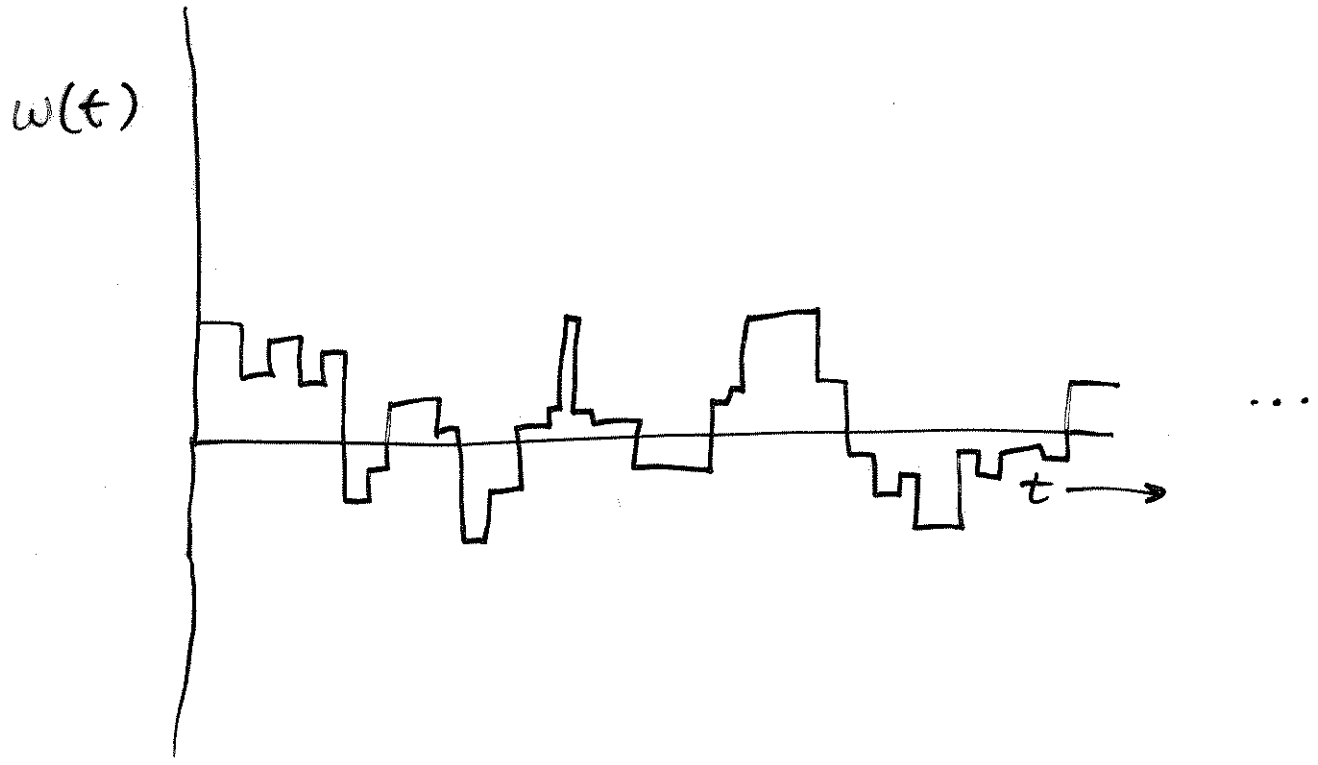

$\exists$ an exact solution for

$$G(t) = \Theta(t)\langle S_+(t) S_-(0)\rangle_{\text{time average}}$$

"NMR absorption spectrum"

for $\omega_i \gtrless \gamma$.

Solutions:

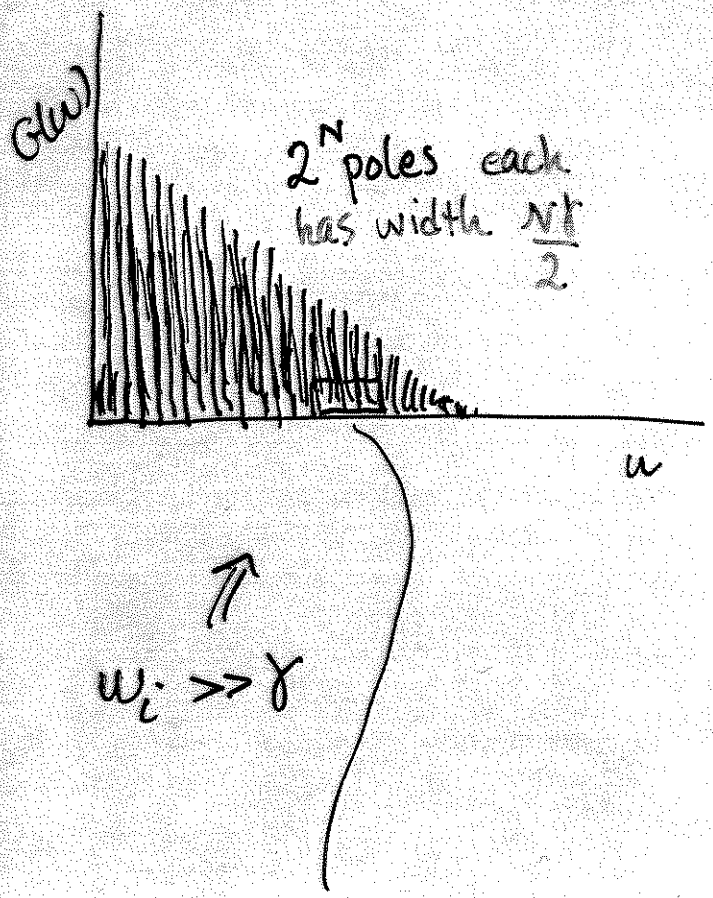

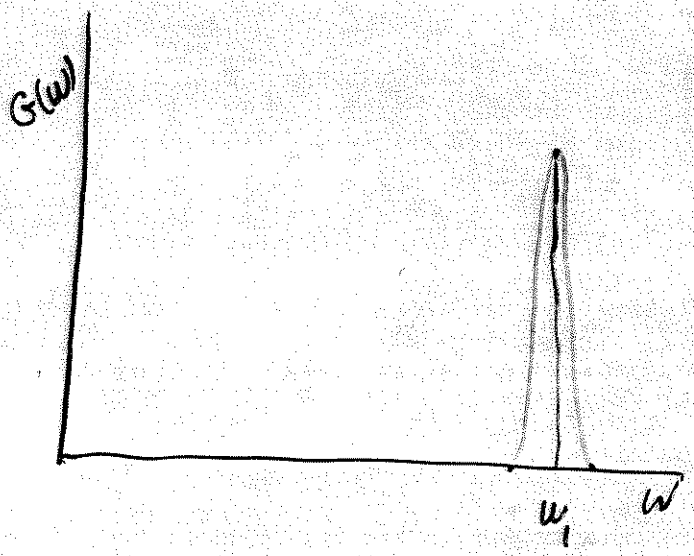

$\omega_1 >> \omega_i \quad i \neq 1$

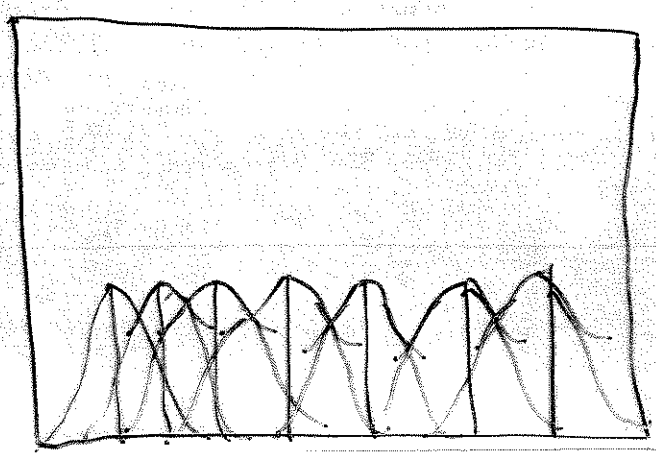

Lots of spectral overlap $\Rightarrow$ "Band".

Analytical solution of model for $\omega_i >> \gamma$:

$$G(\omega) = \sum_{i=1}^{2^N} f(\omega - \Omega_i)$$

Ω_i = possible values of $\omega(t)$

f = Lorentzian of width $N\gamma/2$.

BAND : HOMOG. BROAD. : DELOCALIZED STATES

Solution for $\omega_1 >> \omega_i$ $i \neq 1$:

$$G(\omega) \sim \delta(\omega - \omega_1)$$

LOCALIZED AT SITE.

III. Realistic Calculations

Know how to do inhomo limit [PAIR THEORY]

homo limit [MOMENTS]

What about inbetween ?

When are assumptions of one limit or the other justified ?

Detailed treatment of Dipolar Problem :

(i) HIGH CONCENTRATION ($c \gtrsim .2$) S.C.

almost Every site has at least a few neighbors.

- essentially all spins are in good thermal contact with eachother

$\Rightarrow$ Since these imply that $\exists$ a band

Can use MOMENTS (averaged over config's)

For Dipolar 8 moments are known. But...

Given moments, What is the lineshape?)

i.e. We have to solve the classical Moment problem.

[Given a finite sequence $\{\mu_n\}_{n=0}^{N}$ of moments of $G(\omega) \geq 0$, what G gave rise to μ_n?]

Solution: MAXIMUM ENTROPY INFERENCE ETJ NP LM RC

Find that $G(\omega)$ which maximizes the entropy functional $\mathcal{H} = -\int_a^b G(\omega) \ln G(\omega) \, d\omega$

Subject to known information [moments $\mu_n = \int_a^b dx x^n G(x)$]

" Maxent is least biased in the sense that it makes minimum assumptions about G to give μ_n "

How?

$$\mathcal{H}_{info} = -\int_a^b G(\omega) \log[G(\omega)]\, d\omega \leftarrow \text{Information Shannon / Jaynes entropy}$$

maximize $\mathcal{H}_{info}$ subject to known info:

$$\mathcal{K} = \mathcal{H} + \sum_{i=1}^{N} \lambda_i \left[\mu_i - \int_a^b d\omega\, \omega^n G(\omega) \right]$$

$$\Rightarrow \boxed{G(\omega) = \mathcal{Z}^{-1} \exp\left\{ -\sum_{i=1}^{N} \lambda_i \omega^i \right\}}$$

[Numerical problem: find $\lambda_i \Rightarrow G$ has right moments]

Results for d-d problem (trans)

Lower Concentrations $c \ll .1$

· Expect manifestations of both limits in problem

AN ALGORITHIM:

(i) Simulate dilute lattice with random # generator. (Fix c)

(ii) Assume all spins form a band: Calculate a bandwidth on this assumption

(iii) Check each spin individually:

[if spin is so inhomogeneously broadened that its resonant frequency is outside of bandwidth
Remove it from band (treat with pair theory)

[if spin is well within bandwidth
Keep in band
} treat with moments

iterate

Calculate a lineshape

iterate to convergence

Result :

For dilute limit ($c < 10^{-3}$ on SC lattice) and dipolar (r^{-3}) interaction:

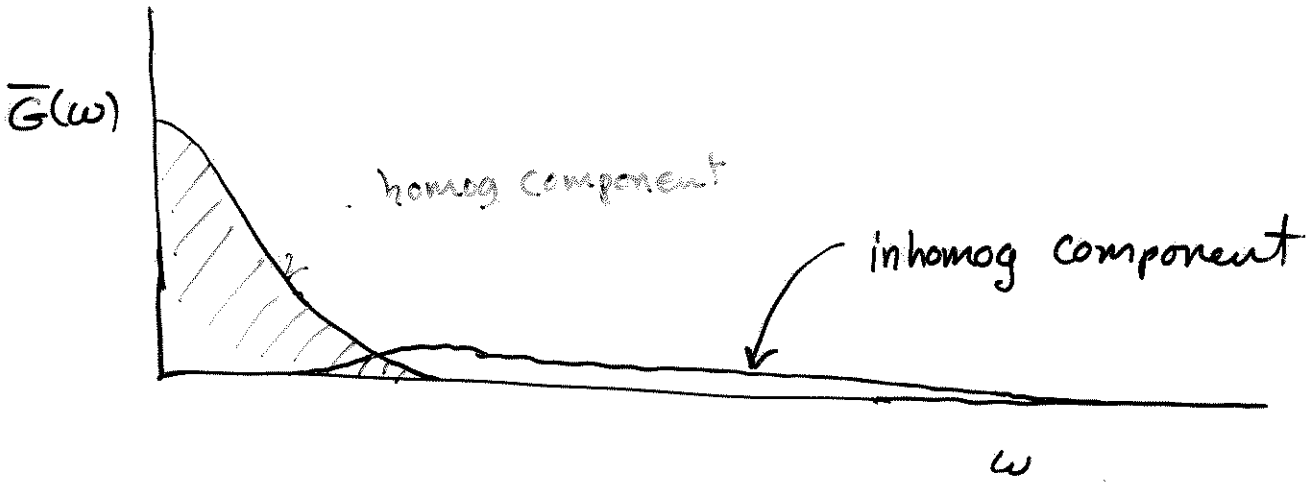

c	% homog
10^{-3}	~12
10^{-2}	~12
10^{-1}	~20
.3	~60
.5	~95

Conjecture: $\exists$ a band for dipolar interaction for any c. Related to dimensionality of space (3) = power of coupling (r^{-3}) ??

Maybe band doesn't exist for $r^{-(3+\varepsilon)}$?

Conclusions for Spin ½

1. $\exists$ a band $\forall c > 0$

2. Assuming either strictly homog. broadening (delocalized) or inhomogeneous broadening (localized) states can lead to grave errors.

3. Maxent is an excellent approach to the moment problem.

IV) Theory of Longitudinal Relaxation for mixtures of ortho ($J=1$) and para ($J=0$) solid hydrogen. [ie- what is T_1 for H nuclear spins ?]

I. Interactions:

Intermolecular (EQQ) between $J=1$ molecules

[Messy bilinear interaction. !]

nuclear - molecular

$$\mathcal{H}_{mn} = \omega_d \sum_{m=-2}^{2} B_{2m} A_{2m}^{\dagger} - \frac{2}{3}\omega_c \sum_{m=-1}^{1} B_{1m} A_{1m}^{\dagger}$$

nuclear spin operators

Molecular Spin operators

Interpret : Normal modes of molecular motions → relaxation of nuclear spins

For temperatures $T \gtrsim 1K$ can neglect effect of nuclear spins on molecular spin, and T_1 is due to transverse molecular spin fluctuations.

in other words, calculation of nuclear T_1 requires only the molecular spin autocorrelation functions

$$G_\alpha(t) = \Theta(t) \langle A_\alpha(i,t)\, A_\alpha^\dagger(i,0) \rangle$$

For <u>high ortho</u> (magnetic : $J=1$) concentration broadening is <u>homogeneous</u> so we can use <u>moments</u> applied to the EQQ Hamiltonian

$$\mathcal{H}_{EQQ} = \sum_{\substack{mn \\ i \neq j}} F_{mn}(ij)\, A_{2m}(i)\, A_{2n}(j)$$

$$F_{mn}(ij) = \frac{\sqrt{70\pi}}{9} \Gamma_0 \left[\frac{a}{r_{ij}}\right]^5 C_{mn}\, Y_4^{n+m}(\Omega_{ij}) \qquad \text{(messy!)}$$

Second moment

$$M_2^\alpha = \text{  } = \sum_{\ell\beta\gamma} |\Omega_{\alpha\beta\gamma}(i\ell)|^2$$

maxent converges to give Gaussian G

$$M_4^\alpha = \text{  }$$

maxent does not converge on $-\infty < \omega < \infty$

to give

$\frac{1}{Z} e^{-\lambda_2\omega^2 - \lambda_4\omega^4}$ - level approximation.

To avoid ad-hockeries [guessing a fitting function]

calculate M_6^α. [trans]

[Maxent converges this time ⇒ Good estimate for T_1

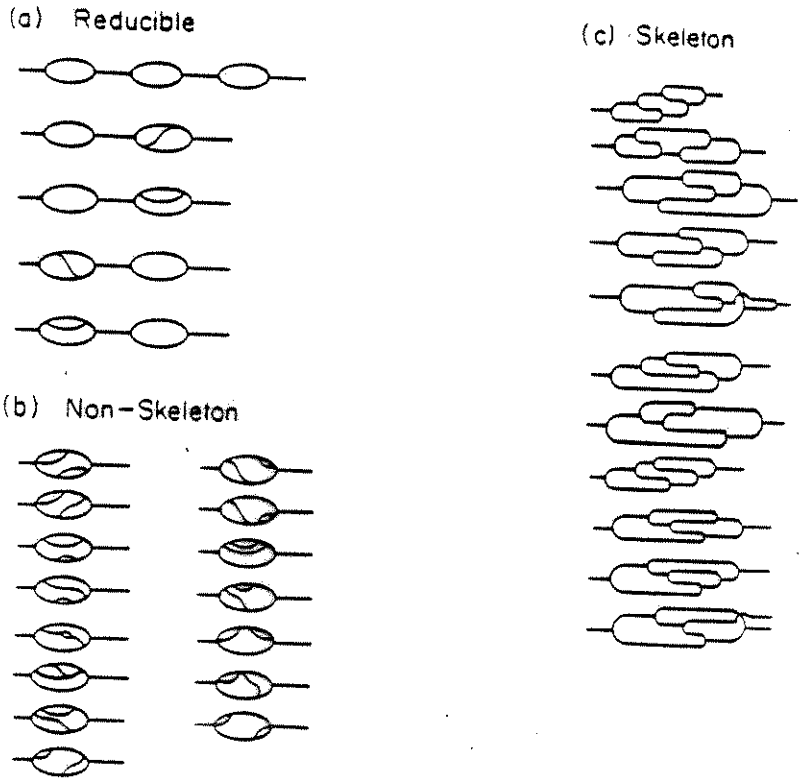

Figure 2. Undecorated graphs required for the sixth moment.

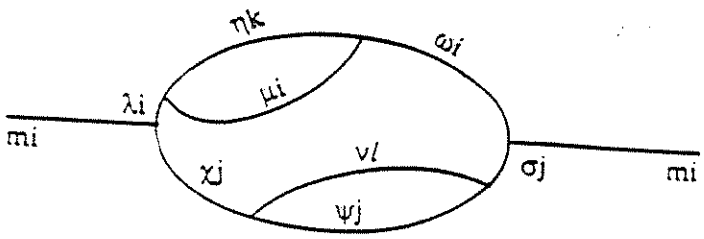

Figure 3. An example of a decorated graph. The analytic expression associated with this diagram is given by Eq. (2).

other than i and m of the analytic expression:

$$\sum_{\substack{-2\le\chi,\eta,\mu,\nu,\sigma\le 2\\ -1\le\omega,\psi,\lambda\le 1\\ <jkl>_{\text{nearest}}\text{neighbors}}} \Omega_{m\lambda\chi}(ij)\Omega_{\lambda\mu\eta}(ik)\Omega_{\chi\psi\nu}(jl)\Omega^*_{\omega\mu\eta}(ik)\Omega^*_{\sigma\psi\nu}(jl)\Omega^*_{m\omega\sigma}(ij) \quad . \qquad (2)$$

The complete sixth moment for $\alpha = (1,m)$ is just the sum of all decorated graphs which start and end with (1,m) lines. The graph of Fig. 3 involves triple sums on sites, so that for o–H_2 concentrations c, each of these diagrams is proportional to c^3. There are actually many graphs which are proportional to c and c^2. Following a procedure first proposed by Abrahams and Kittel,[18] it is then evident that the average moments for the dilute lattice are of the form:

$$\overline{M}_6(c) = \delta c + \varepsilon c^2 + \zeta c^3 \quad . \qquad (3)$$

The sums of the type indicated in Eq. (2) were quite tedious as is evident by the large number of spin and site indexes. In fact, the evaluation of some of these graphs required a supercomputer. All diagrams were evaluated in a nearest neighbor approximation, which has been justified by Hama and Nakamura,[11] and Harris.[10] For c=1 we find that the difference between nearest and second nearest neighbors is ≈1%. This is fortunate, since some of the diagrams would be virtually intractable beyond nearest neighbors.

Hydrogen – low ortho concentration

As usual everbody assumes pair theory or moments to calculate EQQ autocorrelation fcn's.

Nobody can explain c and T dependence of T_1!

Real mechanism: Phonon driven molecular reorientations give rise to c and T dependent modulation of the EQQ induced electric field gradients at o-H_2 sites and this mechanism is dominant for most of available exptl data

⇒ leads to excellent agreement with expt.

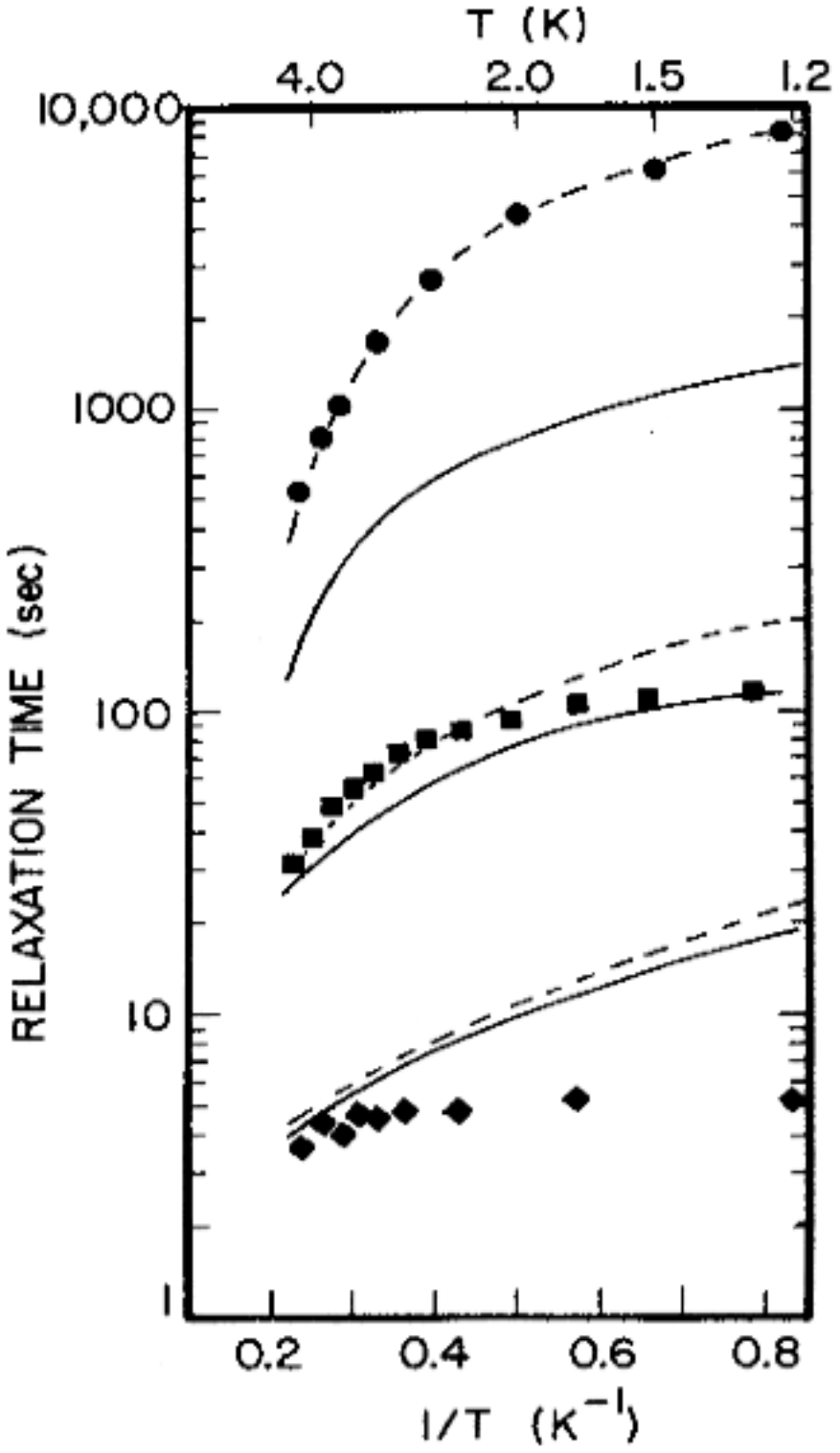

Nuclear spin-lattice relax. of solid HD. DAD and PAF, 1989.

FIG. 5. Comparison of HD relaxation data with theory. Data are from Ref. 5. We illustrate experiment and theory with a subtraction of 5×10^{-5} from n-H_2 concentrations reported in Ref. 5 (dashed line), and the theoretical predictions using the concentrations originally given in Ref. 5 (solid lines). Circles, squares, and diamonds refer to normal concentrations H_2=0.0001, 0.000 28 and 0.0063, respectively, according to Hardy and Gaines.

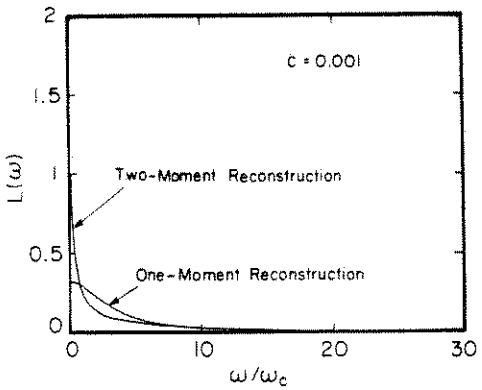

FIG. 1. Strikingly inconsistent line-shape functions for one- and two-moment reconstructions neglecting inhomogeneous broadening at $c=0.001$. In this and all other plots of line shapes, the line shape function is normalized to π, and the frequency is in reduced units of $\omega_c = c\omega_d$, where c is the spin concentration. Although it is difficult to see on this plot, the two moment reconstruction has a value of about 1.8 at the origin.

inhomogeneously broadened).

This works also clearly reflects the existence of a continuum for the dilute limit. We find that for any $\epsilon > 0$, the ratio of the homogeneous population to the total number of spins

$$\lim_{c\to 0} N_{\text{conti}}/N_{\text{total}}$$

is finite for all concentrations (down to $c=0.001$) and depends only on the value of ϵ chosen, and the assumption that the alloy is random. If a continuum did not exist, one could make the limit arbitrarily small by considering a sufficiently dilute lattice. For all very dilute cases we considered ($\epsilon < 0.01$) we found that about 10% of the spins were in the continuum for optimal ϵ.

III. RESULTS AND DISCUSSION

A. High concentrations

In Fig. 2 we present our line shape functions for high concentrations using average moments. For this concentration regime, the line shapes bear some interesting differences. The [100] case is flattened because of the strongly anisotropic dipolar interaction with spins in the first shell. The other two common directions [110] and [111] are much more Gaussian in appearance. We expect the average moment method to be valid for concentrations sufficiently high that isolated configurations are improbable. In practice, for a sc lattice, the great majority of line broadening is continuum in origin down to $c \approx 0.4$. In all graphs of line shape functions, frequencies are measured in units of $\omega_c = c\omega_d$, where ω_d is given in Sec. I. $L(\omega)$ denotes line shape functions in the figures.

B. Low concentrations

For the low-concentration limit, we predict a line width surprisingly consistent with other calculations. The early work of Kittel and Abrahams[15] and Anderson[14] led to half-widths at half maximum of $\delta = 5.3\ \omega_c$ and $\delta = 3.8\ \omega_c$. We predict $\delta \approx 3.7\ \omega_c$, in the notation of our figures. The plots of Fig. 3 are all for the [110] direction and for $c = 10^{-3}$. For low concentrations, the difference in line shapes is negligible for differing Zeeman field configurations—this is a consequence of the dipolar coupling J_{ij} having zero-angle average, and essentially all angles with respect to a given site being attainable for $c \to 0$.

Figure 4 illustrates our method for $c = \frac{1}{10}$ with Zeeman field along the [110] direction. $\epsilon = 0.35$ was again the maximally consistent choice, and about 30% of the spins were in the continuum. For high concentrations the continuum component continued to grow.

It is interesting to compare this work to average moments in the regime where they overlap ($c > 0.3$). For $c = 1$, there is a significant (but tolerable) discrepancy between the self-energy fit to L_2, L_4 and experiment, whereas the three-moment reconstruction almost exactly reproduced experiment.[12] Fortunately, as the concentration decreases, the two-moment fit improves as the continuum part of the line becomes more Gaussian (Fig. 5).

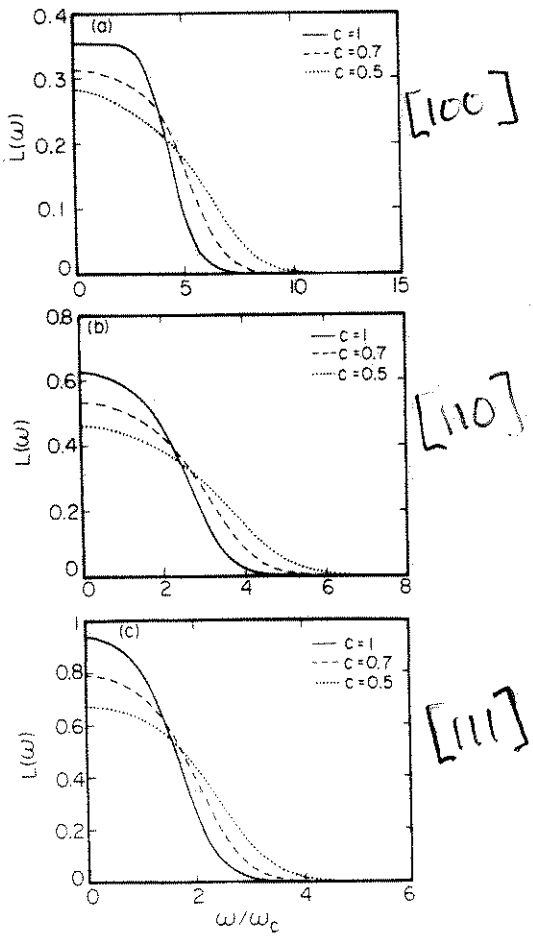

FIG. 2. Line-shape functions at high concentrations and for different Zeeman field configurations. (a) Illustrates the line shapes for the [100] direction, (b) corresponds to [110], and (c) to [111].

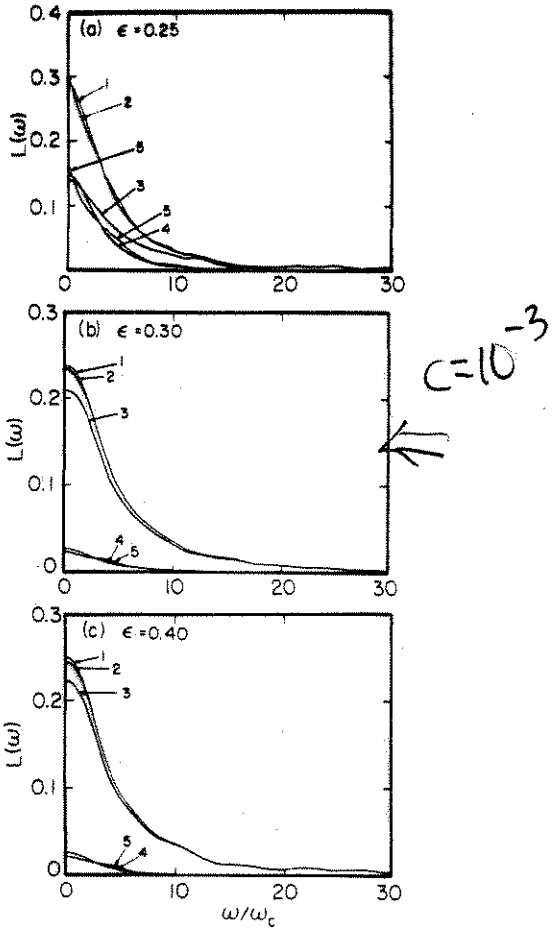

FIG. 3. Line shapes for different ϵ corresponds near the optimally consistent value of 0.35. All plots are for $c=0.001$. (a) Depicts the case of $\epsilon=0.25$, where 37% of the spins are homogeneously broadened. Note the sharp feature in the two moment reconstructions. (b) $\epsilon=0.35$ has 9% of the spins in the continuum. (c) $\epsilon=0.40$ has 6% in the continuum. 1, composite one-moment reconstruction; 2, composite two-moment reconstruction; 3, inhomogeneous; 4, homogeneous one moment; 5, homogeneous two moment.

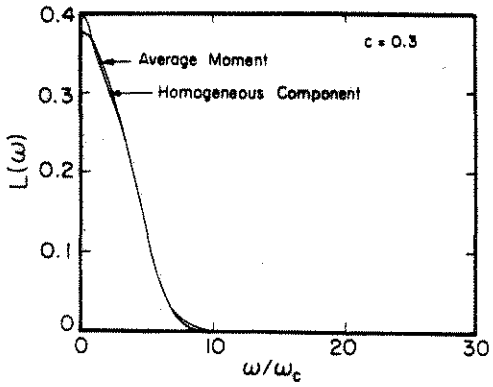

FIG. 5. Comparison of continuum component of line shape and average moments ($c=0.3$, [110]).

As an independent test of our work, we formed the Green's function by diagonalizing the secular dipolar Hamiltonian for several configurations. Because of the prohibitive size of the matrix to diagonalize, even for a moderate number of spins, we present our results only for a very dilute lattice ($c=0.001$), where any particular spin is influenced primarily by a few neighboring spins. We applied periodic boundary conditions to reduce edge effects, and performed the indicated diagonalization for up to nine spins. As we illustrate in Fig. 6, the agreement between the moment analysis and the simulation is reasonable. We are inclined to accept the moment work as the better predicted line shape, since it was computationally feasible to work with many more spins, and easier to configuration average to convergence. The fair agreement between the two methods does suggest that for the dilute limit most of the broadening of the line is inhomogeneous. This is because only inhomogeneous broadening could be well represented by nine or less spins.

C. Discussion

A distinct advantage of simulating randomly diluted lattices is that the investigator is forced to deal with the problem on a configuration by configuration basis. This

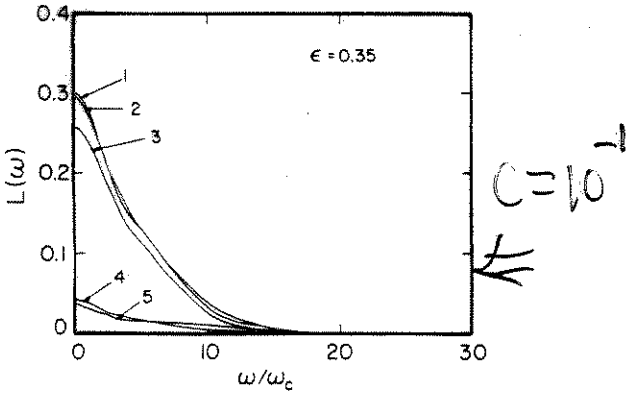

FIG. 4. Line shape for $c=0.1$ and [110]. Here $\epsilon=0.35$, and 15% of the spins are in the continuum. 1, composite one-moment reconstruction; 2, composite two-moment reconstruction; 3, inhomogeneous; 4, homogeneous one moment; 5, homogeneous two moment.

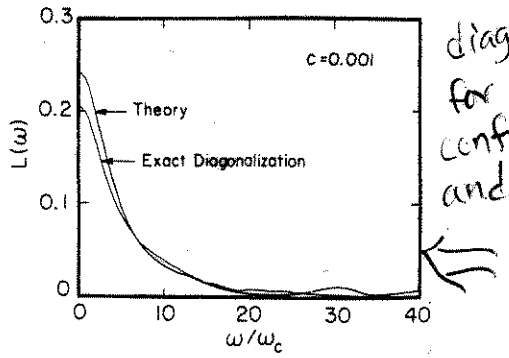

FIG. 6. Comparison of diagonalizing the secular spin-spin interaction, forming the Green's function directly, and the result of our method. Both plots are for $c=0.001$ and the [110] orientation of the Zeeman field.